First Principles Calculation of ε-Phase of Solid Oxygen

K.H. Kamaruddin[a], A.F.Z. Abedin[a], N.A. Zabidi[b,*], M.Z.A. Yahya[a], M.F.M. Taib[c]
and A.N. Rosli[d]

[a]Defence Science Department, Faculty of Defence Science and Technology, Universiti Pertahanan Nasional Malaysia,
Kuala Lumpur 57000, Malaysia

[b]Physics Department, Centre for Defence Foundation Studies, Universiti Pertahanan Nasional Malaysia,
Kuala Lumpur 57000, Malaysia

[c]Faculty of Applied Sciences, Universiti Teknologi MARA, 40450 Shah Alam, Selangor, Malaysia

[d]Faculty of Science and Technology, Universiti Sains Islam Malaysia, Nilai 71800, Negeri Sembilan, Malaysia

The electronic structures of ε-phase of solid oxygen $(O_2)_4$ are studied within the framework of density-functional theory. The intriguing molecule has been known to have magnetic properties at room temperature by applying pressure. Nevertheless, until now there was no evidence of band structure studied in the antiferromagnetic behaviour of $(O_2)_4$. We report a comparison study for spin and non-spin polarization orbital which suggests that this ferromagnetic configuration of $(O_2)_4$ could not be seen experimentally, and antiferromagnetic configuration of $(O_2)_4$ was seen at higher pressure of about 10 GPa. The antiferromagnetic state transforms into the superconducting state as the sample temperature decreases. The results can serve as a useful approximation in studying general features of the electronic structure. The $(O_2)_4$ clusters are reported in the Raman study, having significant absorption at 1516 cm^{-1} below infrared region.

1. Introduction

The diatomic molecule of oxygen with valency configuration of $2s^2p^4$ [1] is one of interest which carries magnetic moment with a spin number $S = 1$ [2]. At present, six phases of solid oxygen having distinct crystallographic properties at different pressure and temperature (P–T) [3, 4] are established unambiguously. A seventh phase has been observed under high pressure but the magnetic interaction which is essential for the molecular arrangement is not well established [5]. As solid oxygen becomes denser, its volume practically decreases while its color becomes darker. Under very high pressure, solid oxygen which can be considered as "spin-controlled crystal" [2] changes its magnetic order [4] and becomes a metal and, at low temperature of 0.6 K, it transforms to a superconducting state, assigned by neutron-diffraction study [6]. The epsilon phase of solid oxygen (ε-O_2) is red in color. It is an intriguing organic compound as compared to the other phases of solid oxygen and exhibits a stable liquid form of oxygen at pressure about 8 GPa [7] at room temperature. The ε-O_2 contains four t_2 molecules and thus forms rhomboid cluster $(O_2)_4$ molecular units [8] which are chemically weakly bonded by the van der Waals forces between O_2 molecules [9, 10]. The crystallography of ε-O_2 was experimentally confirmed to have $C2/m$ (C_{2h}^3) symmetry assigned to the monoclinic structure by powder X-ray [9–11] and single-crystal diffraction [12]. Previous study suggested that ε-O_2 has no long-range magnetic order and shows peculiar behavior as magnetically collapsed [13], where the spin and non-spin polarized orbital calculations were found to have similar total energies [14]. In this paper, we report the electronic band structure and density of states obtained from the first principles electronic structure calculations as well as the vibrational frequency of ε phase of solid oxygen.

2. Materials and method

2.1. Materials

All calculations were made based on experimental structures under high pressure [9, 10]. The structure contains three (C_{2h}^3) symmetry inequivalent atoms; two (oxygen O1 and O2) occupy 4i positions of the monoclinic cell of $C2/m$ space group at $(x, 0, z)$ and the third (O3) at 8j position at (x, y, z). For ease, there are two O_8 clusters in the monoclinic cell. One is placed at the origin of the lattice and the other is at the center of the ab plane. The characterized structure is shown
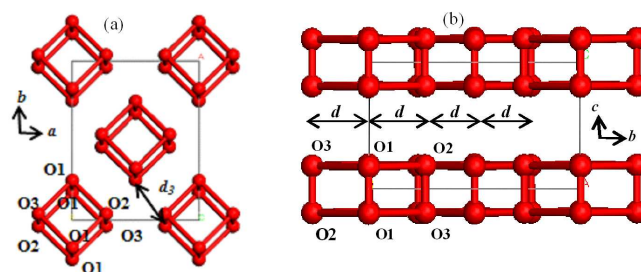

Fig. 1. The ε-O_2 showing (a) a periodic form of $C2/m$ symmetry and (b) the intracluster, d_1 and d_2, as well as the intercluster distances, d_3.

*corresponding author; e-mail: noriza@upnm.edu.my

in Fig. 1a and b at different views and the lattice configurations with atomic coordinates are given in Table I. The electronic band structure obtained at L, M, A, G, Z, and V of k-points was necessary to achieve convergence in the sampling of the Brillouin zone. After optimization at minimum energy, an isolated O_8 cluster is found to have changed in the intracluster distances reported in Table II. The intercluster distances, d_3 are 2.661 Å and 2.610 Å for model 1 and model 2, respectively.

TABLE I

The structural parameters used in the DFT calculation.

Pressure [GPa]		Model 1	Model 2
		11.4	17.6
lattice parameters	a [Å]	8.141	7.77
	b [Å]	5.747	5.501
	c [Å]	3.773	3.657
	β [deg]	117.07	116.4
atomic coordinates	O1	(0.029, 0.266, 0.177)	(0.826, 0, 0.175)
	O2	(0.247, 0, 0.177)	(0.247, 0, 0.192)
	O3	(0.199, 0, −0.177)	(0.0379, 0.2666, 0.185)

TABLE II

The intracluster distances before and after optimization at minimum energy.

Distances	Model 1		Model 2	
	Before [Å]	After [Å]	Before [Å]	After [Å]
O3–O1 (d_1)	2.342	2.074	2.180	2.077
O1–O2 (d_2)	2.349	2.075	2.193	2.077
O1–O1	1.198	1.207	1.203	1.207
O2–O3	1.197	1.207	1.212	1.208

2.2. Methods

Self-consistent electronic structure calculations were performed within the framework of density-functional theory [15, 16] through the Materials Studio (accelrys) package which was based on the all-electron orbital calculations. For most of the calculations, the local density approximation (LDA) and local spin-density approximation in the Perdew and Wang scheme [17] were used to describe the exchange-correlation effect. The generalized gradient approximation (GGA) form of Perdew, Burke and Ernzerhof [18] has been used and the results were found similar to LDA as in the previous studies [19, 20]. Hence, the reported values are only in the LDA. We optimized the structural and lattice parameters for the minimum energy. The vibrational frequency of the isolated cluster of $(O_2)_4$ was obtained at the accuracy of convergence better than 0.01 eV. The total energies of the optimized structures were then determined using the k-point sampling grid along high symmetry directions in the Brillouin zone for primitive unit cell which contains a single unit cell in the lattice structure. The band structure and density of states (DOS) were obtained in the coordinates of k-points:

L (−0.5, 0, 0.5), M (−0.5, −0.5, 0.5), A (−0.5, 0, 0), G (0, 0, 0), Z (0, −0.5, 0.5), and V (0, 0, 0.5).

3. Results and discussion

Figures 2, 3 and 4 show the band structure and density of states of $(O_2)_4$ molecules in Ha unit. The calculations were performed using two different spin configurations. The non-spin polarization was obtained by forcing double occupancy of each band of the models at different pressures. Model 1 (Fig. 2b) shows the Fermi level to lie within the narrow O $2p$ band at 1.02 states/per unit cell of density of states. By allowing unrestricted spin polarized within the unit cell, model 1 of $(O_2)_4$ indicates ferromagnetic material where the bands are found slightly split at the ground state as shown in Fig. 3a and c. The ferromagnetic results of the minority spin state associated with O sites spin up separate from the minority spin down. The spin up are occupied more than the spin down eigenstates. The total energies calculated for spin and non-spin polarized models are found to be essentially the same and therefore the $(O_2)_4$ has been claimed to be nonmagnetic. The phase transforms to nonmagnetic ordered as the sample temperature decreases indicating dissipation of magnetic order [13]. The localized magnetic moments vanished as $(O_2)_4$ materials become superconducting.
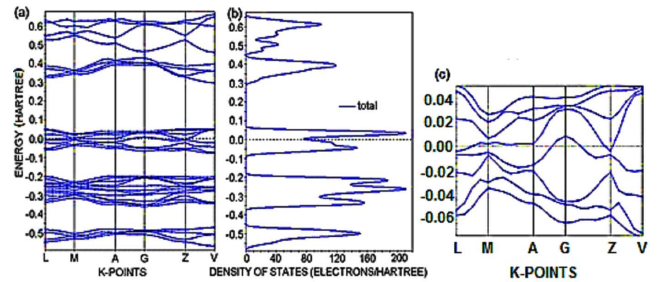

Fig. 2. The (a) band structure, (b) density of states (DOS) and (c) the enlargement of band structure at the Fermi energy, E_F are obtained using non-spin polarized calculation for model 1 at 11.4 GPa.
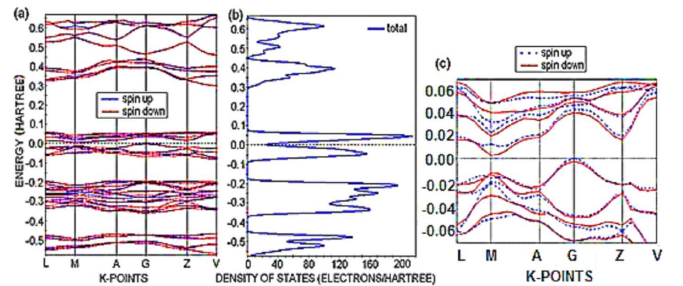

Fig. 3. The (a) band structure, (b) density of states (DOS) and (c) magnified band structure at the Fermi level E_F, results using spin polarized calculation for model 1.

At low pressure, $(O_2)_4$ exhibits a change in behaviour where ferromagnetic materials turn into antiferromagnetic phase (Fig. 4a) as pressure increases, with zero total
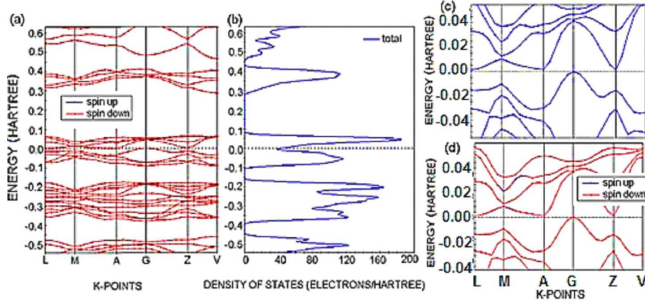
Fig. 4. The (a) band structure, and (b) density of states (DOS) of model 2 calculated by using spin polarized orbitals within LDA. The (c) magnified band structure of non-spin polarized, and (d) the magnified band structure of spin polarized calculation at Fermi level E_{F}.

magnetization in the absence of external magnetic field. The result shows only the plot of spin up contributions, since spin down distribution is identical with the spin up. The antiferromagnetic is obtained by forcing opposite spins on sites related by inversion symmetry within the unit cell, consistent with experimental antiferromagnetic structure at low temperature. The indirect band gaps for model 1 as shown in Fig. 2c are 0.025 eV at M–L, 0.185 eV at M–A and 0.446 eV at V–Z. We find the minimum indirect gap energy of G–A at 0.044 eV for model 2 (Fig. 4c) to be approximately similar to the one established in theoretical study [21] which performed pseudopotential plane-wave method in the calculation. The direct gaps results for both models are given in Table III.

TABLE III

The direct energy gaps of models 1 and 2 at different k-points symmetry.

	L	M	A	G	Z	V
Model 1 energy [eV]	0.083	0.1902	0.4762	0.6164	0.083	1.7763
Model 2 energy [eV]	0.4735	0.5667	0.8716	1.1282	0.4735	2.4513

Further, the observed Raman spectra in ε-O_2 phase have fewer vibrational modes as shown in Fig. 5. Only G-point is used when performing electron–phonon dispersion in the Raman study. The vibrational modes were calculated for an ε-O_2 phase which is found to reach significant absorption at 1512 cm^{-1} for model 1 (Fig. 5a) and 1516 cm^{-1} for model 2 (Fig. 5b) similarly to the Raman values in previous study [8]. The higher peak of model 1 (Fig. 5a) shows two frequencies having the same value which contributes to degeneracy, as compared to the model 2 (Fig. 5b) which shows two significant frequency and results in one highest peak which give useful information in determining various characteristics of their structure.
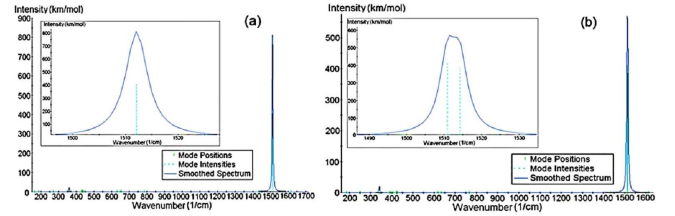

Fig. 5. The vibrational frequency of (a) model 1 (the higher peak shows two frequencies having the same value contributing to degeneracy, shown in inset), and (b) model 2 (the higher peak showing two different frequencies, shown in inset).

4. Conclusion

We have calculated the band gaps of ε-O_2 phase for which p band has the greatest electron density at the Fermi surface. At higher pressure, it is found that in the DOS the structure exhibits metallic behaviour under normal state and becomes superconducting under cooling at high temperature, while at lower pressure, 10 GPa, the structure exhibits ferromagnetic behaviour. There exists coupling between molecules causing the magnetic moments to switch from one molecule to the other. This results in the occurrence of antiferromagnetic material at higher pressure.

References

[1] D. Vandebilt, *Phys. Rev. B* **41**, 7892 (1990).

[2] Y.A. Freiman, H.J. Jodl, *Phys. Rep.* **401**, 1 (2004).

[3] Y. Akahama, H. Kawamura, O. Shimomura, *Phys. Rev. B* **64**, 054105 (2001).

[4] I.N. Goncharenko, O.L. Makarova, L. Ulivi, *Phys. Rev. Lett.* **93**, 055502 (2004).

[5] T. Nomura, Y.H. Matsuda, S. Takeyama, A. Matsuo, K. Kindo, J.L. Her, T.C. Kobayashi, *Phys. Rev. Lett.* **112**, 247201 (2014).

[6] R.J. Meier, R.B. Helmholdt, *Phys. Rev. B* **29**, 1387 (1984).

[7] M. Nicol, K. Syassen, *Phys. Rev. B* **28**, 1201 (1983).

[8] F.A. Gorelli, L. Ulivi, M. Santoro, R. Bini, *Phys. Rev. Lett.* **83**, 4093 (1999).

[9] L.F. Lundegaard, G. Weck, M.I. McMahon, *Nature* **443**, 201 (2006).

[10] H. Fujihisa, Y. Akahama, H. Kawamura, Y. Ohishi, O. Shimomura, H. Yamawaki, M. Sakashita, Y. Gotoh, S. Takeya, K. Honda, *Phys. Rev. Lett.* **97**, 085503 (2006).

[11] Y. Akahama, H. Kawamura, D. Häusermann, M. Hanfland, O. Shimomura, *Phys. Rev. Lett.* **74**, 4690 (1995).

[12] G. Weck, P. Loubeyre, R. LeToullec, *Phys. Rev. Lett.* **88**, 035504 (2002).

[13] I.N. Goncharenko, *Phys. Rev. Lett.* **94**, 205701 (2005).

[14] J.B. Neaton, N.W. Ashcroft, *Phys. Rev. Lett.* **88**, 205503 (2002).

[15] P. Hohenberg, W. Kohn, *Phys. Rev.* **136**, B864 (1964).

[16] W. Kohm, L.J. Sham, *Phys. Rev.* **140**, A1133 (1965).

[17] J.P. Perdew, Y. Wang, *Phys. Rev. B* **45**, 13244 (1992).

[18] J.P. Perdew, K. Burke, M. Ernzerhof, *Phys. Rev. Lett.* **77**, 3865 (1996).

[19] A.N. Rosli, N.A. Zabidi, H.A. Kassim, K.N. Shrivastava, *J. Cluster Sci.* **21**, 197 (2010).

[20] N.A. Zabidi, H.A. Kassim, K.N. Shrivastava, *AIP Conf. Proc.* **1017**, 326 (2008).

[21] Y.-H. Liu, Z.-M. Liu, Y.-M. Ma, Z. He, F.-B. Tian, T. Cui, B.-B. Liu, G.-T. Zou, *Chin. Phys. Lett.* **24**, 11 (2007).